Synthesis and Excited-State Photodynamics of Perylene-Bis(Imide)-Oxochlorin Dyads. A Charge-Separation Motif

Christine Kirmaier,[†] Eve Hindin,[†] Jennifer K. Schwartz,[†] Igor V. Sazanovich,[†] James R. Diers,[‡] Kannan Muthukumaran,[§] Masahiko Taniguchi,[§] David F. Bocian,*[,‡] Jonathan S. Lindsey,*[,§] and Dewey Holten*[,†]

Department of Chemistry, Washington University, St. Louis, Missouri 63130-4899, Department of Chemistry, University of California, Riverside, California 92521-0403, and Department of Chemistry, North Carolina State University, Raleigh, North Carolina 27695-8204

Received: September 8, 2002; In Final Form: January 2, 2003

Three perylene-oxochlorin dyads have been prepared and characterized with the goal of identifying charge-injection or molecular-switching motifs for use in molecular photonics. Each dyad consists of a perylene-bis(imide) dye (PDI) joined at the 10-position of a magnesium, zinc, or free base (Fb) oxochlorin via a diphenylethyne linker. Each dyad has been studied in both polar and nonpolar media using static and time-resolved optical spectroscopy and electrochemical techniques. Dyad PDI−MgO is an excellent charge-separation unit in which the excited perylene (~3.5 ps lifetime) or the excited oxochlorin (lifetimes of 0.5 ns in benzonitrile and 1.0 ns in toluene) give rise to state PDI^- MgO^+ in high overall yield (>90%); the charge-separated state has a lifetime of ≥1 ns in both toluene and benzonitrile. The pathway for generating PDI^- MgO^+ from the excited perylene (PDI*) involves both hole transfer and energy transfer to the oxochlorin followed by electron transfer from the resulting MgO* to PDI. Similar decay of PDI* by energy transfer and hole transfer is found for dyads PDI−ZnO and PDI−FbO. However, electron-transfer quenching of the excited oxochlorin in these two dyads either does not occur or occurs to a much lesser degree than for PDI−MgO in both polar and nonpolar solvents. For PDI−FbO the decay of the charge-separated state occurs significantly by charge recombination to give the excited oxochlorin, making this a good light-harvesting system even though the early stages of the dynamics include charge separation/recombination. The observed differences in the extent of the possible excited-state processes (energy, hole, and electron transfer) among the dyads and in polar versus nonpolar media are consistent with the estimated energy ordering of the excited- and charge-separated states. This study has provided a new class of arrays containing perylene accessory pigments and oxochlorin chromophores that can be utilized for applications in light harvesting and molecular optoelectronics.

Introduction

One theme of our recent work has been the design, synthesis, and characterization of molecular architectures containing porphyrins or porphyrins plus accessory pigments that undergo facile energy- and/or charge-transfer processes in a controlled manner.[1] Efficient excited-state energy transfer is critical for light harvesting while charge-transfer processes underlie opto-electronic gating. Recently we have shown that arrays containing perylenes and porphyrins can be designed to select for excited-state energy or charge transfer by tuning the redox and photophysical properties of the components.[2−12] We have also begun to extend our studies of tetrapyrroles by developing new synthetic routes to chlorins[13−15] and oxochlorins,[16] an area of active research in recent years.[17] A number of dyads containing chlorins/oxochlorins or one of these chromophores with an accessory pigment or electron acceptor have been prepared.[18−36]

In the preceding paper, we showed that a dyad consisting of a perylene-monoimide dye and a zinc oxochlorin joined by a diphenylethyne linker is an excellent light-harvesting motif: energy is transferred rapidly and effectively quantitatively from the perylene component to the oxochlorin unit, the excited state of which subsequently decays with characteristics comparable to those of the isolated chromophore.[37] In the present paper, we utilize instead a perylene-bis(imide) accessory pigment, the prototypical unit being PDI-1 shown in Chart 1. We have previously utilized this dye in diphenylethyne-linked dyads containing a zinc, magnesium, or free base porphyrin (PDI−ZnP, PDI−MgP, and PDI−FbP; Chart 1). In the present paper, we have prepared and studied the analogous oxochlorin dyads PDI−ZnO, PDI−MgO, and PDI−FbO (Chart 1). The goal is to utilize the favorable redox characteristics of both units and the enhanced red absorption of the oxochlorins (compared to porphyrins) to elicit both strong light absorption over a broad region and efficient generation of long-lived charge-separated states. The dyads have been characterized by electrochemistry, static absorption, and fluorescence spectroscopy, and time-resolved fluorescence and transient absorption spectroscopy. Taken together, the studies described herein provide fundamental insight into the design and function of dyad architectures for specific applications in molecular photonics.

* To whom correspondence should be addressed. (Dewey Holten) E-mail: holten@wuchem.wustl.edu. (Jonathan S. Lindsey) E-mail: jlindsey@ncsu.edu. (David F. Bocian) E-mail: David.Bocian@ucr.edu.
[†] Department of Chemistry, Washington University.
[‡] Department of Chemistry, University of California.
[§] Department of Chemistry, North Carolina State University.

10.1021/jp0269423 CCC: $25.00
Published on Web 03/20/2003

CHART 1

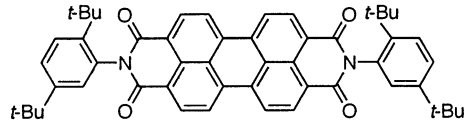

PDI-1

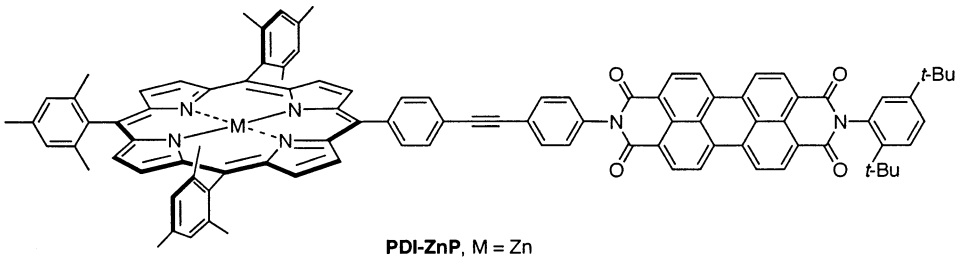

PDI-ZnP, M = Zn

PDI-MgP, M = Mg

PDI-FbP, M = H, H

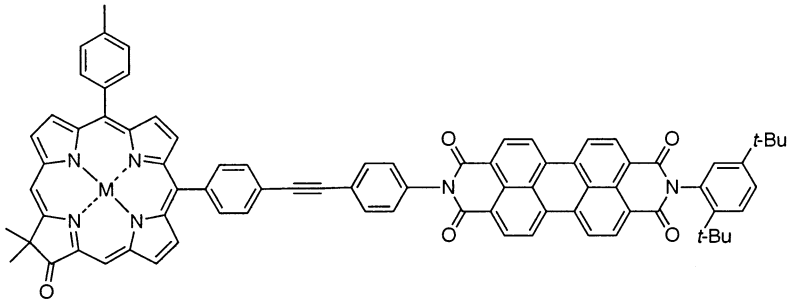

PDI-ZnO, M = Zn

PDI-MgO, M = Mg

PDI-FbO, M = H, H

Results and Discussion

Synthesis. The rational synthesis of C-alkylated chlorins provides ready access to a variety of chlorin building blocks.[13−15] We recently developed a simple procedure for oxidation of the methylene group in the reduced ring of the chlorin, forming the corresponding oxochlorin.[16] Thus, treatment of zinc chlorin Zn1[13,14] with basic alumina (activity I) in toluene at 50 °C in the presence of air gave a mixture of the zinc hydroxychlorin and a trace amount of the zinc oxochlorin. The mixture was then treated with 2,3-dichloro-5,6-dicyano-1,4-benzoquinone (DDQ) in toluene for 5 min to give the desired zinc oxochlorin ZnO1 in 47% overall yield (Scheme 1).

The perylene-Zn-oxochlorin dyad was synthesized by the Pd-catalyzed coupling of the ethynylphenyl-substituted zinc oxochlorin and the iodo-substituted perylene building block. The coupling reactions were carried out under similar conditions developed for joining porphyrins,[2,3] which have been used recently for attaching perylenes to porphyrins.[4,6,7,8] The conditions employ dilute solutions of the reactants in the presence of tris[dibenzylideneacetone]-dipalladium(0) [$Pd_2(dba)_3$] and tri-*o*-tolylphosphine [P(*o*-tol)$_3$] in a solution of toluene/triethylamine (TEA) at 35 °C. Thus, the Pd-mediated reaction of ethyne-substituted ZnO1 and *N*-(2,5-di-*tert*-butylphenyl)-*N*′-(4-iodophenyl)-3,4,9,10-perylenetetracarboximide (PDI-2)[6] afforded the perylene-bis(imide)-Zn-oxochlorin dyad PDI−ZnO in 51% yield (Scheme 1). The dyad PDI−ZnO was characterized by laser desorption mass spectrometry, ^{1}H NMR spectroscopy and absorption spectroscopy. The demetalation of PDI−ZnO using trifluoroacetic acid (TFA) in CH_2Cl_2 afforded the corresponding free-base dyad PDI−FbO in 76% yield. Treatment of PDI−FbO with MgI_2 in CH_2Cl_2 in the presence of *N*,*N*-diisopropylethylamine (DIEA) at room temperature (heterogeneous method for magnesium insertion)[38] afforded the Mg-containing dyad PDI−MgO in 45% yield.

Several oxochlorin benchmarks were prepared from ZnO1. Demetalation of ZnO1 on treatment with TFA in CH_2Cl_2 afforded the free-base chlorin FbO1 in 94% yield (Scheme 2). Magnesium insertion was achieved by treating FbO1 with MgI_2 and DIEA to afford MgO1 in 92% yield. Each oxochlorin in this series bears one ethyne group.

Electrochemical Characterization. The electrochemical data for dyad PDI−ZnO and benchmark perylene dye PDI-1 are summarized in Table 1. The $E_{1/2}$ values were obtained with square wave voltammetry (frequency 10 Hz). The isolated perylene dyes exhibit one oxidation and two reduction waves in the +1.4 to −2.0 V range. As we have previously reported,[5,7] the redox potentials of the perylene-bis(imide) dyes studied here are anodically shifted by ∼0.4 V relative to those of the perylene-monoimide dyes studied in the preceding article.[37] The $E_{1/2}$ values for the perylene units in the dyads are generally similar to those of the isolated dyes. The oxochlorin unit in each of the dyads exhibits two oxidation and two reduction waves in the +1.4 to −2.0 V range; the $E_{1/2}$ values are similar to those of the monomeric macrocycle (ref 16 and J. R. Diers

SCHEME 1

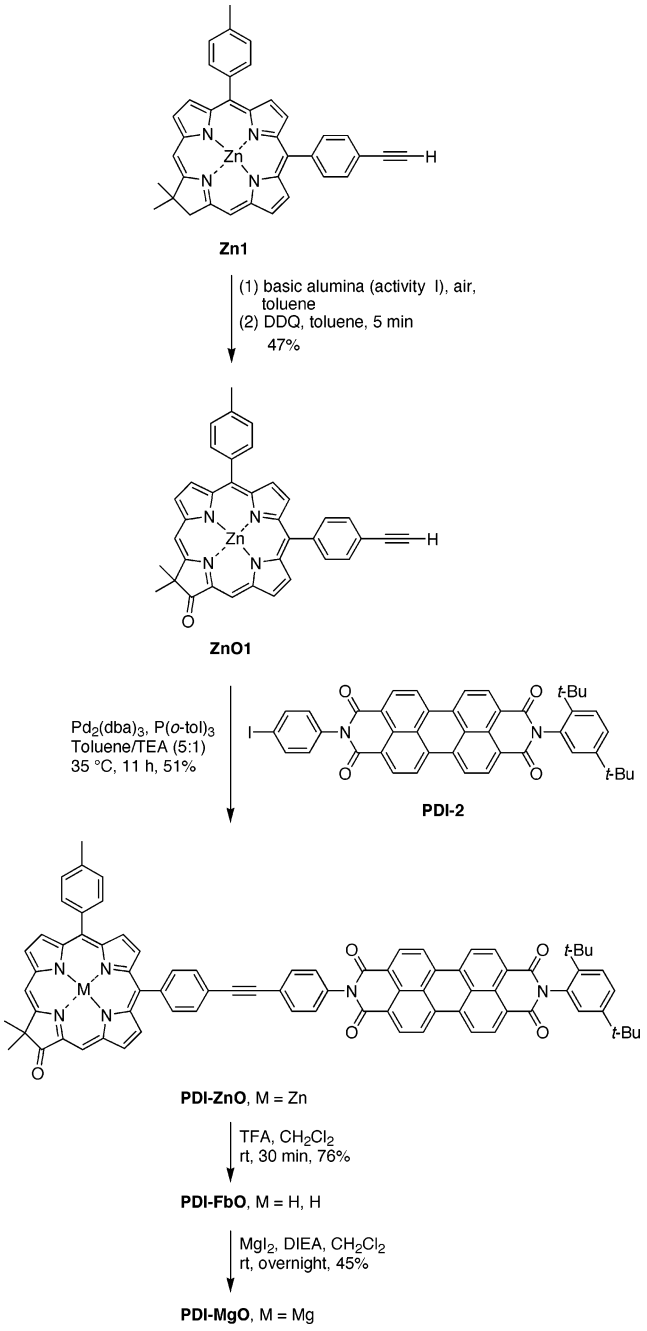

SCHEME 2

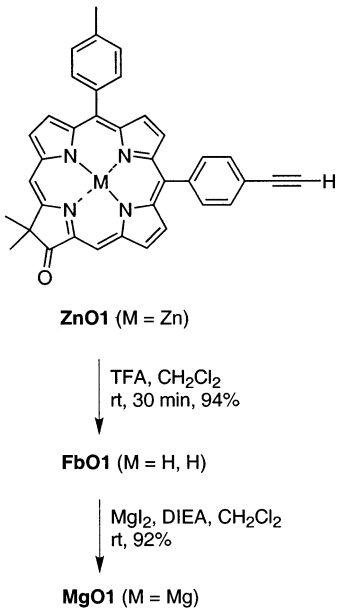

TABLE 1: Half-Wave Potentials ($E_{1/2}$)[a]

	oxidation potentials			reduction potentials			
		oxochlorin		perylene		oxochlorin	
	perylene	$E_{1/2}$ (1)	$E_{1/2}$ (2)	$E_{1/2}$ (1)	$E_{1/2}$ (2)	$E_{1/2}$ (1)	$E_{1/2}$ (2)
PDI-1[b]	+1.36			−0.81	−1.07		
PDI−ZnO	+1.40[c]	+0.51	+0.75	−0.76	−1.04	−1.56	−1.94
ZnO[d]		+0.59	+0.89			−1.50	n.m.[e]

[a] Obtained in butyronitrile containing 0.1 M $(n\text{-Bu})_4NPF_6$. $E_{1/2}$ vs Ag/Ag^+; $E_{1/2}$ of $FeCp_2/FeCp_2^+ = 0.19$ V. The $E_{1/2}$ values are obtained from square wave voltammetry (frequency = 10 Hz). Values are ± 0.01 V. [b] Taken from ref 7. [c] Value is approximate because the maximum in the redox wave is outside the electrochemical window. [d] For an oxochlorin monomer described in the preceding paper (ZnO9).[37] [e] Not measured.

and D. F. Bocian, unpublished results). The similarity of the redox potentials of the components of the dyads with that of the isolated components is indicative of the relatively weak ground-state electronic interactions between the dyad components.

Photophysical Properties. Complete photophysical characterization of each of the three perylene-oxochlorin dyads depicted in Chart 1, as well as of the reference monomers, was carried out in toluene and in benzonitrile at room temperature. Studies were performed in these two solvents because potential applications may utilize the arrays in either nonpolar or polar media. The static absorption and emission spectra of each dyad and all of the photophysical properties of each reference compound generally differ only modestly in the two solvents. These effects are due mainly, but not exclusively, to the coordination of benzonitrile to the central metal ion in the Zn- and Mg-containing oxochlorins. The most significant difference in photophysical properties of a given dyad in the two solvents is that benzonitrile provides greater energy stabilization of the charge-separated states (e.g., involving the oxidized oxochlorin and reduced perylene), which can alter the rates and yields of the excited-state processes. These effects are illustrated in Figure 1, which summarizes the excited-state processes that have been deduced from this study. Reference to this summary diagram will aid in the presentation and discussion of the results.

Absorption Spectra. The ground-electronic-state absorption spectrum of each perylene-oxochlorin dyad is essentially given by the sum of the spectra of the subunits, reflecting relatively weak perylene-oxochlorin interactions. This point is illustrated in Figure 2 for PDI−ZnO in toluene (solid spectra). The absorption spectrum is dominated by the oxochlorin near-UV Soret band at ∼425 nm, the oxochlorin $Q_y(0,0)$ band ($S_0 \rightarrow S_1$) at ∼610 nm, and the perylene absorption contour ($S_0 \rightarrow S_1$) between 450 and 550 nm. The spectrum of PDI−ZnO and the PDI-1 reference monomer contains a clear vibronic progression with an origin at 527 nm. Spectra analogous to those shown in Figure 2 are given in the Supporting Information for PDI−ZnO (and its reference monomers) in benzonitrile as well as for PDI−MgO and PDI−FbO in both solvents. For comparison purposes, spectra focused on the PDI and oxochlorin origin bands (500−660 nm) for the three dyads and both solvents are shown in Figure 3. In all three dyads, the blue-green absorption of the

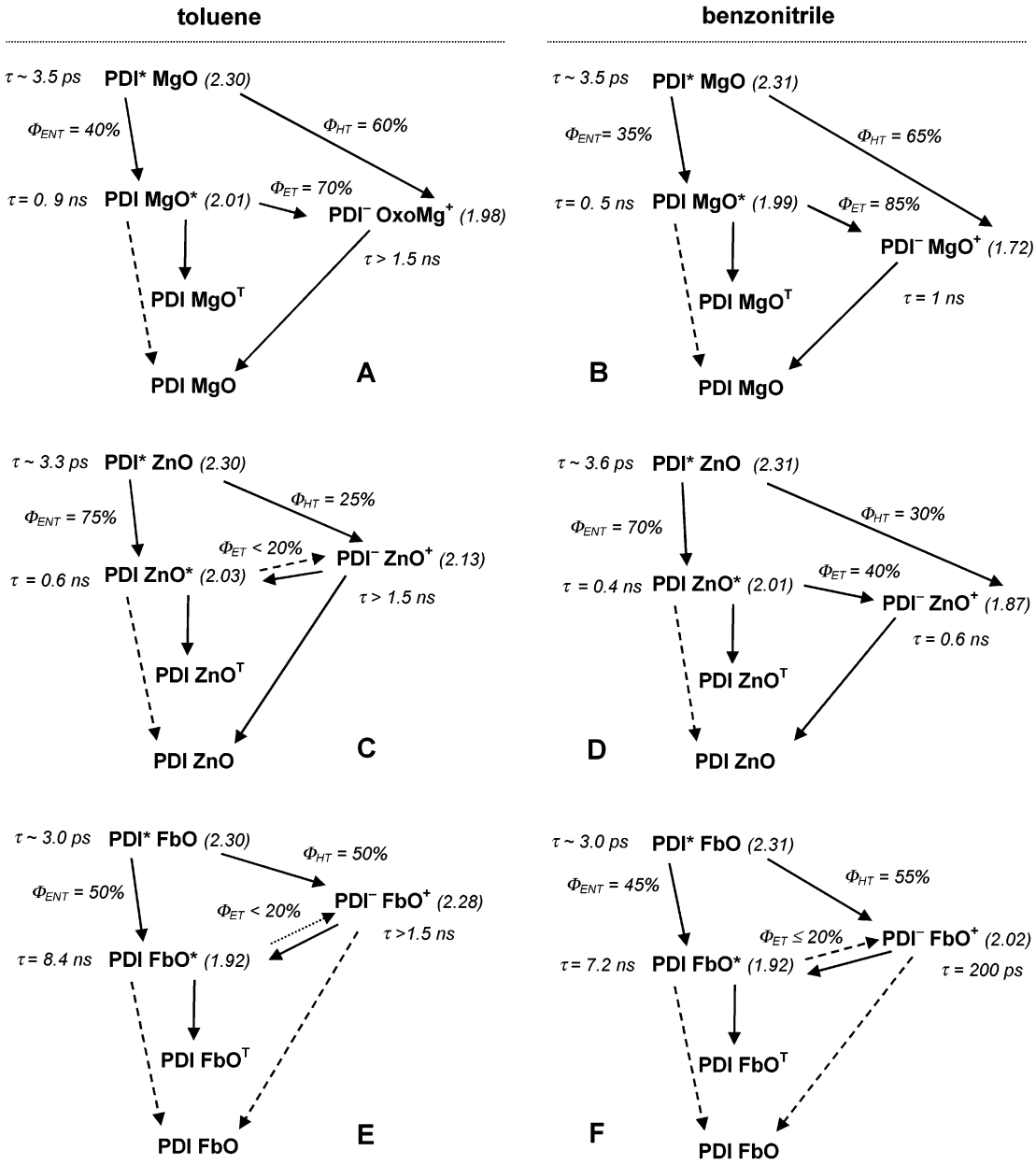

Figure 1. Summary diagram showing the excited-state processes in the dyads at room temperature. The values in parentheses are the estimated free energies of the states in eV (see text).

perylene accessory pigment complements the blue and red absorption of the oxochlorin, thereby giving broad spectral coverage.

Fluorescence Spectra and Quantum Yields. Fluorescence emission spectra for PDI−ZnO and its reference monomers in toluene at room temperature are shown in Figure 2 (dashed and dotted spectra). Fluorescence spectra for all the dyads and reference monomers in both toluene and benzonitrile are given in the Supporting Information. Excitation of the perylene subunit of PDI−ZnO in toluene at 480 nm produces a substantial amount of oxochlorin emission, namely, the (0,0) band at 612 nm and the (0,1) band at 670 nm (Figure 2A, dotted spectrum) that are at the same positions found for the ZnO1 monomer (Figure 2B). The level of the oxochlorin emission is a sizable fraction of that found with direct oxochlorin excitation at 392 nm (Figure 2A, dashed). This finding is indicative of significant energy transfer from the excited perylene (PDI*) to the ground-state oxochlorin to form ZnO*. The emission spectrum obtained using primarily perylene excitation also contains perylene emission, as indicated by the bands at ∼540 and ∼580 nm (Figure 2A, dotted) that lie at the same positions as in the PDI-1 monomer (Figure 2C). This perylene emission in PDI−ZnO is reduced by orders of magnitude from that in the monomer, reflecting the fact that PDI* decays predominantly by a combination of energy and hole transfer to the oxochlorin, with relative yields that are best determined from the transient absorption data described below (see Figure 1C). The fact that residual perylene emission is observed in the dyad despite the substantial quenching derives from the high intrinsic emission yield of this chromophore (Table 2), as we described in the previous article for PMI−ZnO.[37]

The oxochlorin emission yields for PDI−ZnO, PDI−MgO, and PDI−FbO in toluene and benzonitrile were determined from the spectra obtained with direct oxochlorin excitation (see Figure 2A, dashed), with subtraction of the residual perylene emission followed by comparison to a fluorescence standard (FbTPP), as described in the previous paper.[37] The resulting yields are given in Table 2, along with those for the benchmark monomers.

TABLE 2: Photophysical Data for Perylene-Oxochlorin Dyads and Reference Compounds[a]

		PDI* decay		O* decay			PDI$^-$ O$^+$ decay
compound	solvent	τ (ps)[b]	Φ_{HT}[c]	Φ_f[d]	τ (ns)[e]	Φ_{ET}[f]	τ (ns)[g]
dyads							
PDI−MgO	toluene	3.5	0.60	0.032	0.9 ± 0.2	0.70 ± 0.05	>1.5
	benzonitrile	3.5	0.65	0.011	0.5 ± 0.2	0.85 ± 0.05	1.0 ± 0.3
PDI−ZnO	toluene	3.3	0.25	0.030	0.6 ± 0.2	<0.2	>1.5
	benzonitrile	3.6	0.30	0.018	0.4 ± 0.1	0.4 ± 0.2	0.6 ± 0.2
PDI−FbO	toluene	3.0	0.50	0.10	8.4 ± 0.5	<0.2	>1.5
	benzonitrile	3.0	0.55	0.080	7.2 ± 0.5	<0.2	0.20 ± 0.05
monomers							
MgO1	toluene			0.13	3.1 ± 0.2		
	benzonitrile			0.14	3.0 ± 0.2		
ZnO1[h]	toluene			0.037	0.7 ± 0.2		
	benzonitrile			0.030	0.7 ± 0.2		
FbO1	toluene			0.13	9.0 ± 0.5		
	benzonitrile			0.13	9.1 ± 0.5		
PDI-1	toluene	3600[i]		0.97[i]			
	benzonitrile	3800		0.99			

[a] All data at room temperature. [b] Lifetime of the perylene lowest excited singlet state; the values for the dyads were determined by transient absorption spectroscopy (average single-exponential fit through the PDI bleaching region) and those in the monomers by fluorescence decay (±200 ps). [c] Yield of hole transfer to the oxochlorin (±5%); the corresponding yield of energy transfer is $\Phi_{ENT} \sim 1 - \Phi_{HT}$. [d] Oxochlorin fluorescence yield (±15%) determined using Soret (392 nm) excitation and free base tetraphenylporphyrin (FbTPP) in toluene ($\Phi_f = 0.11$) as a standard.[41] The yield for PDI-1 in benzonitrile was referenced to the value in toluene. [e] Oxochlorin excited-singlet-state lifetime determined by averaging the values determined by transient absorption kinetics and fluorescence decay. [f] Yield of electron transfer from excited oxochlorin to perylene determined by averaging the values obtained from transient absorption spectra, excited-state lifetimes, and fluorescence yields (see text). [g] Decay of the charge-separated state involving the reduced perylene and oxidized oxochlorin. [h] Similar values are obtained for other zinc oxochlorin monomers.[37] [i] From ref 5.

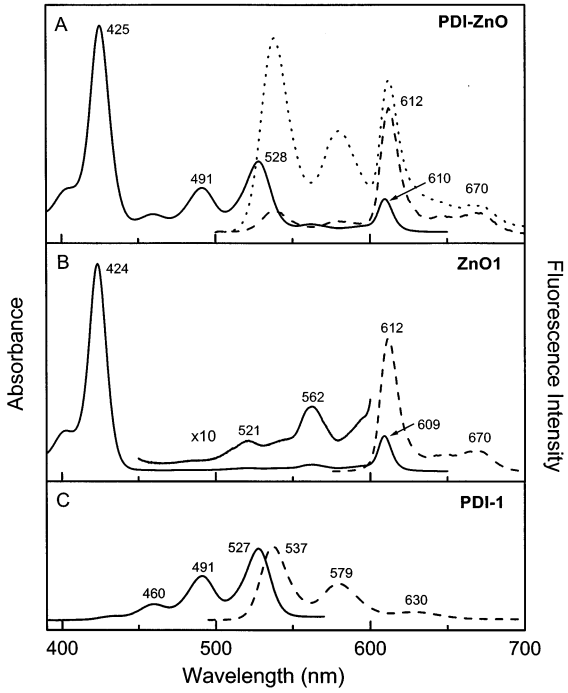

Figure 2. Absorption spectra (solid) and fluorescence spectra (dashed, dotted) at room temperature. Emission for the dyad was obtained using primarily excitation of the porphyrin at 392 nm (dashed) or perylene at 480 nm (dotted). The emission intensities in parts A and B have been corrected for the absorbance at the excitation wavelength and on the same scale so that they can be compared. The intensities in C have been reduced by an order of magnitude for clarity of presentation.

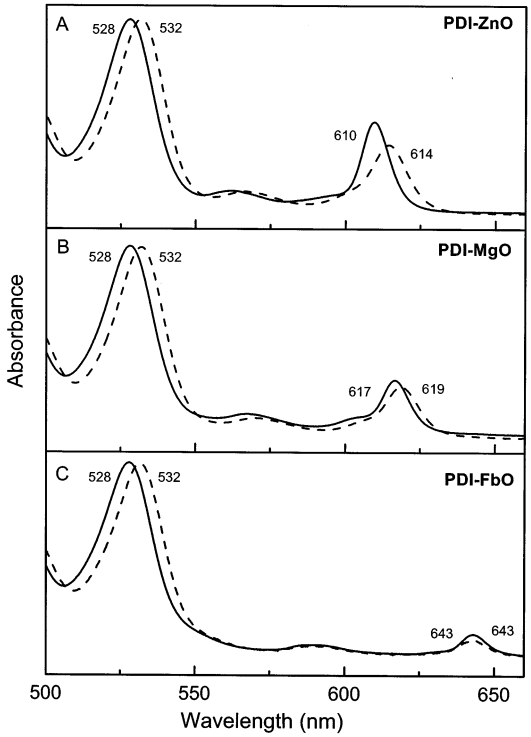

Figure 3. Ground-state absorption spectra in the region of the perylene and oxochlorin origin bands in toluene (solid) and benzonitrile (dashed) at room temperature.

A substantial reduction in fluorescence yield in the dyad compared to the monomer is found for PDI−MgO in both solvents. As indicated by the analysis given below, this quenching is indicative of substantial electron transfer from MgO* to the perylene in this dyad (Figure 1A,B).

Fluorescence Lifetimes. A second assay of the extent of oxochlorin charge-transfer quenching in each dyad is obtained from comparison of the excited-singlet-state lifetime with that of the appropriate reference compound in the same solvent. The excited-state lifetimes can be determined by both fluorescence and time-resolved absorption techniques; the latter measurements are described in the following section. Both methods were used for each of the metallooxochlorin-containing dyads and for monomer ZnO1 (in both toluene or benzonitrile), and the average values for each solvent are given in Table 2. The lifetimes for these compounds derived from multiple determina-

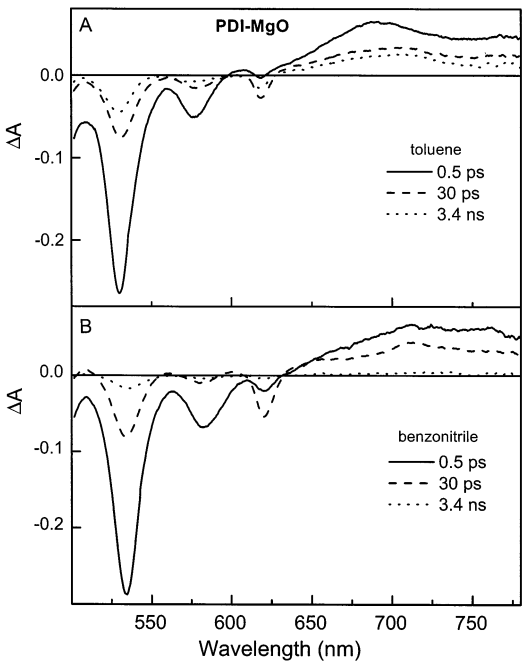

Figure 4. Transient absorption spectra at selected pump−probe delay times for dyad PDI−MgO in (A) toluene and (B) benzonitrile following excitation with a 130 fs flash at 495 nm.

tions using fluorescence modulation spectroscopy are as follows: PDI−ZnO in toluene (0.6 ± 0.1 ns) and benzonitrile (0.4 ± 0.1); PDI−MgO in toluene (0.9 ± 0.2 ns) and benzonitrile (0.6 ± 0.2 ns); ZnO1 in toluene (0.8 ± 0.2 ns) and benzonitrile (0.7 ± 0.2 ns). These fluorescence lifetimes are generally somewhat longer than those obtained by transient absorption, but agree within the error limits of the average values given in Table 2. The excited-state lifetimes listed in Table 2 for PDI−FbO, FbO1, and MgO1 were obtained from fluorescence measurements alone. It should be noted that the fluorescence measurements on some dyads/solvents indicate the presence of a second, minor component. This component generally could be attributed to minor (free) perylene emission ($\tau = 3-5$ ns). However, in some cases this second component may represent the decay of a charge-separated state (involving oxidized oxochlorin and reduced perylene) by charge recombination to give in part the oxochlorin excited singlet state (see Figure 1).

Time-Resolved Absorption Spectra. The presentation of the transient absorption data for the three perylene-oxochlorin dyads will be facilitated by reference to Figure 1, which summarizes the collective results on the excited-state photodynamics of these systems.

PDI−MgO. Figure 4 shows time-resolved absorption difference spectra for PDI−MgO in toluene (part A) and benzonitrile (part B) at selected pump−probe time delays. The results are generally similar for this dyad in the two solvents, so the two cases will be presented together. In each solvent, the initial (0.5 ps) spectrum was constructed from a series of spectra acquired at very closely spaced time intervals in order to account for the time-dispersion of wavelengths in the white-light probe pulse (Figure 4A,B, solid). This initial spectrum can be associated primarily with the excited perylene (PDI*) produced by direct perylene excitation at 495 nm. The pronounced feature at ∼530 nm contains bleaching of the perylene ground-state (0,0) absorption band (see solid spectrum in Figure 2C) and (0,0) stimulated (by the white-light probe pulse) emission from PDI* that occurs in the same region as the spontaneous fluorescence (see dashed spectrum in Figure 2C). The PDI* spectrum also shows a broad excited-state absorption band centered at ∼690 nm.

The early-time dynamics of PDI* in PDI−MgO in both toluene and benzonitrile shows evidence for both relaxation (conformational, vibrational, or electronic) and subsequent decay of the relaxed form of the excited state. This behavior is analogous to that described in the preceding article for the excited perylene PMI* in dyad PMI−ZnO (although there are differences in detail).[37] One indication of these two contributions to the PDI* dynamics is a probe wavelength variation in a simple single-exponential fit through the data at times <50 ps ($\tau \sim 2-7$ ps), as is shown for PDI−MgO in benzonitrile (Figures 5A-C). It is possible that both the relaxed and unrelaxed forms of PDI* in PDI−MgO participate in energy/hole transfer to the oxochlorin, which itself may undergo excited-state relaxation on the 1−10 ps time scale.[16] Thus, in assessing the overall rates of these processes, we will utilize an effective PDI* lifetime of 3.5 ps derived from the PDI bleaching decay (Table 2).

After PDI* has decayed, the perylene feature at ∼530 nm has diminished (but not disappeared) and the oxochlorin (0,0) bleaching plus stimulated emission feature at ∼620 nm has developed to its maximum amplitude (Figure 4A,B, dashed). The spectrum at 30 ps in either toluene or benzonitrile cannot be ascribed solely to the excited oxochlorin (MgO*) formed by perylene-to-oxochlorin energy transfer because the latter state would show no perylene bleaching. Hence, the residual perylene bleaching must reflect partial decay of PDI* by perylene-to-oxochlorin hole transfer to give PDI^- MgO^+ (which will give perylene bleaching). The amplitude of the perylene (0,0) bleaching at 30 ps compared to the (approximately equal) bleaching plus stimulated emission for PDI* at 0.5 ps indicates that the yield of PDI* hole-transfer is ∼60% in toluene and slightly larger in benzonitrile. The energy-transfer pathway primarily governs the other fraction of PDI* decay (Figure 1A,B and Table 2). The relative amplitudes of the perylene and oxochlorin features in the transient difference spectra of PDI−MgO (Figure 4) are consistent with these interpretations and with the features in the static optical spectra (see Figure 3 and Supporting Information) when allowance is made for modest transient absorption in the 500−630 nm region (no larger than that seen at >700 nm).

The above analysis shows that PDI* decays to give both MgO* and PDI^- MgO^+ for PDI−MgO in both solvents. Thus, one expects to observe the decay of both of these states, with the former possibly giving rise to an additional amount of the latter by electron transfer (depending on the relative energy ordering of the states). The changes in the transient absorption spectra between 30 ps and 3.4 ns give evidence for these processes. Note that the decay of MgO* and PDI^- MgO^+ will have the same sign of $\Delta\Delta A$ at most wavelengths while the growth of the latter state will generally have the opposite sign. Kinetic analysis shows that the MgO* and PDI^- MgO^+ lifetimes are similar. The combination of these phenomena give rise to complex kinetic profiles that require dual-exponential fitting at times >50 ps at some wavelengths, and a probe wavelength dependence of a single-exponential fit at other wavelengths. The representative kinetic traces shown in Figure 5 illustrate these points. Detailed analysis gives best dual-exponential fits across the 500−730 nm region with time constants of 0.9 ns and ≥1.5 ns for PDI−MgO in toluene and 0.5 and 1.0 ns in benzonitrile.

The most consistent assignment based on the spectra and the fluorescence lifetime and yields is that the shorter time constant reflects the lifetime of MgO* and that the longer value is due

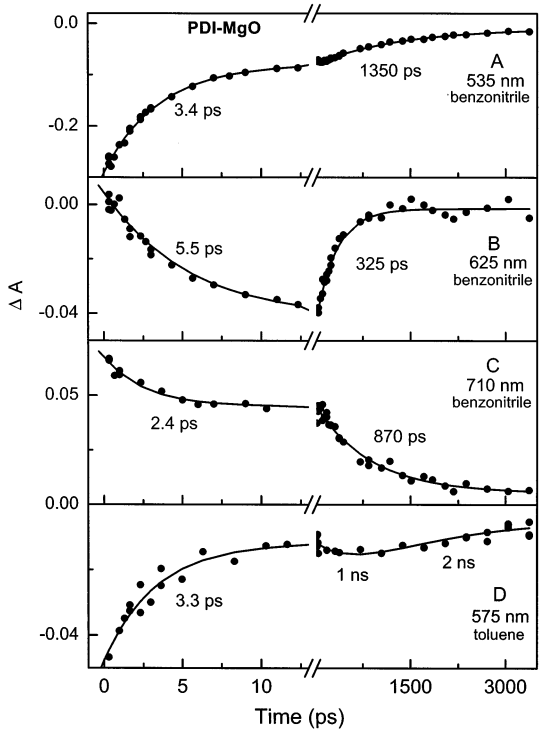

Figure 5. Kinetic traces and multiexponential fits at selected wavelengths for PDI−MgO. Parts A−C show results from the same measurements in Figure 4B and in part D from those in Figure 4A.

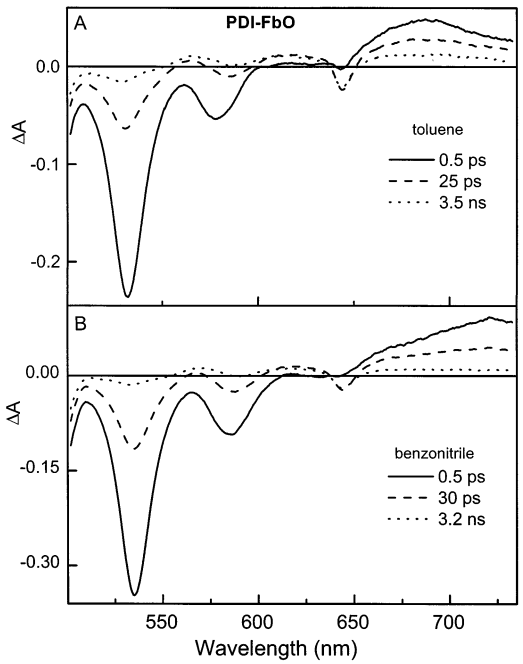

Figure 6. Transient absorption spectra at selected pump−probe delay times for dyad PDI−FbO in (A) toluene and (B) benzonitrile following excitation with a 130 fs flash at 483 nm.

to decay of PDI^- MgO^+. The data also suggest that the latter state forms in high yield from the former in both solvents, complementing the amount of the charge-separated state produced directly from PDI* (Figure 1A,B). The fact that the PDI^- MgO^+ requires ≥1.5 ns to decay in toluene is seen directly from the transient difference spectrum at 3.4 ns in Figure 4A (dotted). This spectrum shows a significant amount of both perylene and oxochlorin bleaching and thus cannot be assigned simply to ZnO^T (formed from ZnO*), which would show no perylene bleaching. In benzonitrile, more of the spectrum has collapsed to the baseline by 3.4 ns (Figure 4B, dotted). This result indicates that MgO* has been severely quenched by electron transfer to the perylene and that charge recombination of PDI^- MgO^+ is almost complete by 3.4 ns in the polar medium. The rate constants and yields of the various processes consistent with all of the time-resolved and static optical data for PDI−MgO will be derived below (Table 2).

PDI−FbO. Transient absorption difference spectra for PDI−FbO in toluene and in benzonitrile obtained using primarily excitation of the perylene at 483 nm are shown in Figure 6. In analogy to the spectra for PDI−MgO (Figure 4), the spectrum in each solvent at 0.5 ps can be ascribed to PDI* (Figure 6, solid). Relaxations within this excited state and decay of the relaxed form give rise to two components in the early-time (<50 ps) dynamics (Figure 7A,B), with an average PDI* lifetime of ∼3 ps in each solvent determined from single-exponential fits to the PDI bleaching (Table 2). Also in analogy to PDI−MgO, the spectrum at 30 ps shows both perylene and oxochlorin bleachings that arise from a combination of FbO* and PDI^- FbO^+ formed from PDI* decay. The amplitude of the PDI feature at ∼530 nm at 30 ps versus 0.5 ps indicates that the yield of the charge-separated state via the PDI* hole-transfer pathway is ∼50% in toluene and slightly higher in benzonitrile, with the other fraction of the PDI* decay occurring by the energy-transfer route (Table 2 and Figure 1E,F).

At this point the analogies between the behavior of PDI−FbO and PDI−MgO end. In both toluene and benzonitrile, the PDI bleaching present at 30 ps (due to state PDI^- FbO^+) decays substantially by 3.4 ns, but the oxochlorin bleaching plus stimulated emission at ∼640 nm changes only modestly. This observation suggests that the charge-separated state PDI^- FbO^+ that is formed from PDI* decays largely by charge recombination to form the excited oxochlorin (FbO*) with only modest return to the ground state. Based on the PDI bleaching decay at ∼530 nm that occurs between ∼30 ps and 3.4 ns (and the kinetics in other regions such as ∼700 nm where PDI^- absorbs), the time constant for charge recombination is ∼200 ps in benzonitrile and >1.5 ns (likely 2−4 ns) in toluene (Figures 7A and 7B and Table 2). The spectral features remaining at 3.4 ns can be ascribed primarily to FbO*, which according to the fluorescence measurements decays with a time constant only slightly shorter than the lifetime of 9 ns for the isolated oxochlorin (Table 2).

PDI−ZnO. Figure 8 shows selected transient absorption data for dyad PDI−ZnO using primarily excitation of the perylene at 495 nm. The elucidation of the excited-state processes for this dyad proved to be the most difficult of all the arrays because the data ultimately show a significantly higher yield of perylene-to-oxochlorin energy transfer and an intermediate yield of electron-transfer quenching of the excited oxochlorin. Therefore, studies were also carried out using excitation flashes at 540 nm (excites both the perylene and oxochlorin components) and 585 nm (excites primarily oxochlorin). The results and conclusions summarized in the following are most consistent with all the measurements. The PDI* decay again shows evidence for two components ($\tau \sim 2.5-7.0$ ps) associated with decay of the unrelaxed and relaxed forms (see Figure 7C,D), with an average PDI* lifetime of ∼3.5 ps determined by single-exponential decays of the PDI bleaching in both toluene and benzonitrile (Table 2). The extent of PDI bleaching (∼530 nm) at 30 ps compared to bleaching plus stimulated emission at 0.5 ps affords a yield of ∼25% for PDI* ZnO → PDI^- ZnO^+ hole transfer in toluene, giving a yield of 75% for PDI* ZnO →

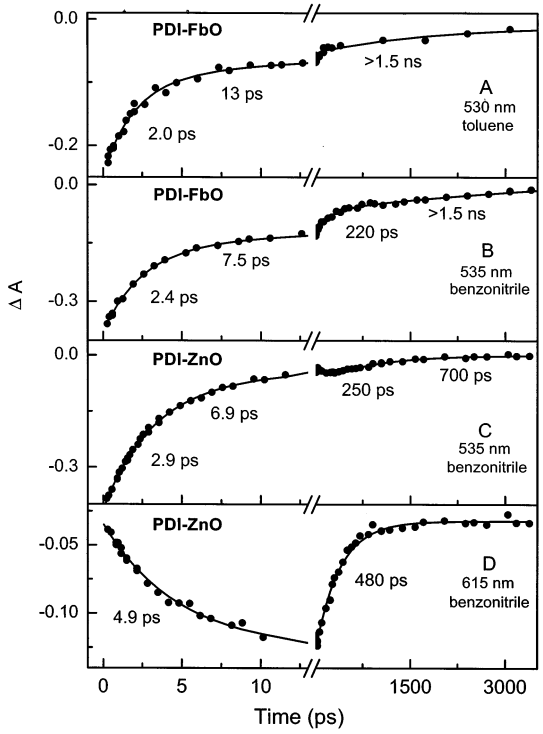

Figure 7. Kinetic traces and multiexponential fits at selected wavelengths for PDI−FbO from the same measurements shown in (A) Figure 6A or (B) Figure 6B or for PDI−ZnO from the same measurements shown in (C and D) Figure 8B.

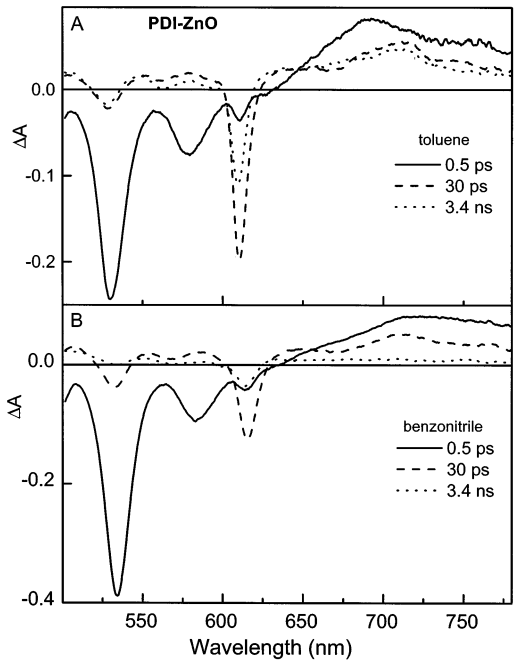

Figure 8. Transient absorption spectra at selected pump−probe delay times for dyad PDI−ZnO in (A) toluene and (B) benzonitrile following excitation with a 120 fs flash at 495 nm.

PDI ZnO* energy transfer; in benzonitrile, the hole transfer yield is slightly larger and the energy transfer slightly less than in toluene (Table 2). In toluene, there is little decay of the PDI bleaching at ∼530 nm between 30 ps and 3.4 ns (Figure 8A, dashed and dotted spectra), indicating that PDI^- FbO^+ has a lifetime >1.5 ns (likely 3 ns). The PDI^- ZnO^+ bleaching decays with a time constant of 600 ± 200 ps in benzonitrile, as deduced from measurements across the spectrum (500−800 nm) using 495 or 540 nm excitation. One of the complexities is that ZnO* also decays on this time scale, so that the spectral changes contain a convolution of the decay of the oxochlorin excited state, decay of PDI^- ZnO^+ formed from PDI*, and possibly the formation and subsequent decay of the PDI^- ZnO^+ formed from ZnO* (see Figure 1C,D). Figure 7C,D show two examples of the resulting kinetic traces that either clearly show two kinetic components or an intermediate time constant from a single-exponential fit (which is probe wavelength dependent) on the 30 ps to 3.4 ns time scale. Combined analysis of the transient absorption and fluorescence measurements give a ZnO* lifetime for PDI−ZnO of 0.6 ns in toluene and 0.4 ns in benzonitrile (Table 2).

Energies of the Electronic States of the Dyads. In constructing the state diagrams shown in Figure 1, the energies of the excited perylene and porphyrin components were taken directly from the spectroscopic data for each dyad. In particular, the average energies of the (0,0) absorption and fluorescence bands of the two components of each array were used to obtain the energies of the lowest excited singlet states (Figure 1). The free energies of the charge-separated states were derived using an experimentally determined[5] reference value of 2.05 eV for state PDI^- ZnP^+ in the perylene-porphyrin dyad PDI−ZnP in toluene (the porphyrin analogue of PDI−ZnO) along with appropriate differences in ground-state redox potentials (using the assumptions and methods described previously[6]) as follows (Figure 1). (1) State PDI^- ZnO^+ in PDI−ZnO is 80 meV higher than PDI^- ZnP^+ in PDI−ZnP due to the ∼80 mV more positive oxidation potential of zinc oxochlorins versus zinc porphyrins (Table 1 and refs 6 and 16). (2) State PDI^- FbO^+ in PDI−FbO and PDI^- MgO^+ in PDI−MgO are 150 meV higher and lower, respectively, than PDI^- ZnO^+ in PDI−ZnO using the +150 mV and −150 mV typical differences in oxidation potentials of Fb and Mg porphyrins, respectively, versus Zn porphyins.[6] (3) The charge-separated species will be stabilized by 0.26 eV in benzonitrile versus toluene; this value was estimated using the simple Coulomb interaction $e^2/(\epsilon_s r)$, where e^2 = 14.45 eV·Å), r is the oxochlorin-perylene center-to-center separation (∼21 Å), and ϵ_s is the static dielectric constant (2.38 for toluene and 25.2 for benzonitrile).

Rates and Yields of the Energy- and Charge-Transfer Processes. The transient absorption data described above have provided the relative yields of the two principal decay pathways of the excited perylene (PDI*) in each dyad, namely energy or hole transfer to the oxochlorin (Figure 1 and Table 2). These pathways cause the excited perylene in each dyad to have a lifetime that is about 3 orders of magnitude shorter than the lifetime of ∼5 ns for the isolated dye, with an average value (unrelaxed and relaxed forms) of 3−4 ps (Table 2). The rate constants and yields for decay of the excited perylene in the PDI-based dyads can be obtained by applying standard methods, taking into account the branching ratio for energy versus hole transfer.[5]

For PDI−MgO in toluene, the transient absorption data indicate that the fractional yields of the energy- and hole-transfer pathways are 0.40 and 0.60, respectively. Using the PDI* lifetimes for the dyad and MgO1 monomer in Table 2, the overall rate constant for combined quenching of PDI* by energy plus hole transfer is $k_Q = [(3.5\text{ ps})^{-1} - (4500\text{ ps})^{-1}]^{-1} \sim (3.5\text{ ps})^{-1}$ with an overall quenching yield of $\Phi_Q = 1-3.5/4500 \sim 99.9\%$. Thus the rate constant and quantum yield for PDI* MgO → PDI MgO* energy transfer are $k_{ENT} = [(3.5\text{ ps})^{-1}][0.40] = (8.7\text{ ps})^{-1}$ and $\Phi_{ENT} = (0.40)(0.999)(100) = 40\%$, while the values for PDI* MgO → PDI^- MgO^+ hole transfer are $k_{HT} = [(3.5\text{ ps})^{-1}][0.60] = (5.8\text{ ps})^{-1}$ and $\Phi_{HT} = (0.60)(0.999)(100)$

= 60%. The rate constants and yields for the principal decay pathways for the other PDI-based dyads in toluene or benzonitrile are similarly obtained (Figure 1 and Table 2). The finding that each of the PDI-based dyads (PDI−FbO, PDI−ZnO, and PDI−MgO) exhibits significant hole transfer is consistent with the energy estimates given above in which the charge-separated state is placed lower in free energy than PDI* (Figure 1). This behavior contrasts that observed in the preceding article for PMI−ZnO, which showed little or no evidence of hole transfer, consistent with the prediction that PMI^- ZnO^+ is above PMI* in free energy.[37]

The transient absorption spectra have provided insights into whether the excited oxochlorin in each dyad/solvent decays by electron transfer to the perylene in addition to the normal routes open to the isolated chromophore (mainly intersystem crossing to the excited triplet state). However, assessment of the extent of electron transfer also can be provided by comparison of the lifetime and fluorescence yield of the excited oxochlorin in the dyad compared to the values in the reference monomers using standard equations.[5]

The excited oxochlorin in PDI−MgO undergoes extensive electron transfer to the perylene in both polar and nonpolar media. The MgO* lifetime for the dyad in toluene (0.9 ns) compared to the MgO1 reference monomer (3.1 ns) gives an electron-transfer yield for PDI MgO* → PDI^- MgO^+ of $\Phi_{ET} = 1-0.9/3.1 = 0.71$ (Table 2). A value of $\Phi_{ET} = 1-0.032/0.13 = 0.75$ is obtained from the corresponding fluorescence yields (Table 2), giving a conservative estimate of 0.70. For PDI−MgO in benzonitrile, the corresponding calculations based on the MgO* lifetimes and fluorescence yields afford $\Phi_{ET} = 1-0.5/3.0 = 0.83$ and $\Phi_{ET} = 1-0.011/0.13 = 0.91$ giving a conservative estimate of 0.85 (Table 2). It should be noted that the high yield of the charge-separated state from MgO* supplements the yield of 60% in toluene and 65% in benzonitrile from PDI* (with the remaining fraction of PDI* forming MgO*). Thus, the ultimate yield of PDI^- MgO^+ beginning in PDI* is 60% + (40% · 0.7) ∼ 88% in toluene and 65% + (35% · 0.85) ∼ 95% in benzonitrile. The high yields of electron transfer (PDI MgO* → PDI^- MgO^+) are generally consistent with the estimates that place the latter state comparable in energy to the former in toluene and well below it in benzonitrile (Figure 1). In addition to the high yields of electron transfer, the transient absorption data indicate that PDI^- MgO^+ has a lifetime of ∼1 ns or longer in both solvents. Thus, PDI−MgO is well suited for incorporation into more elaborate arrays as a molecular-switching or charge-injection unit.

The excited perylene in PDI−ZnO and PDI−FbO also serves effective roles as a parallel light-harvesting and hole-transfer agent. Using the PDI* lifetimes and the yields of the two pathways given in Table 2, rate constants comparable to those found above for PDI−MgO are obtained. This is expected given that each of the charge-separated states PDI^- ZnO^+ and PDI^- FbO^+ lies below PDI*, consistent with the energy estimates (Figure 1). One of the principal differences among the dyads is the extent to which ZnO* in PDI−ZnO or FbO* in PDI−FbO in toluene or benzonitrile is quenched by electron transfer to the perylene to also produce the charge-separated state. On the bases of fluorescence quantum yields and excited-state lifetimes in Table 2, the only one of these four cases (two dyads and two solvents) for which some electron transfer is clear is PDI−ZnO in benzonitrile. Using the same analysis methodology described above, the quantum yield of electron-transfer based on the lifetime or fluorescence yield in the dyad versus monomer is $\Phi_{ET} = 1 - 0.4/0.7 = 0.4$ or $\Phi_{ET} = 1 - 0.018/0.030 = 0.4$ (Table 2). This level of electron transfer is not sufficient for an effective charge-separation unit, although the finding of electron transfer is consistent with the energy estimates that place PDI^- ZnO^+ slightly below ZnO* in benzonitrile. The excited-state lifetimes and fluorescence yields for PDI−ZnO in toluene and PDI−FbO in either solvent are very similar in the dyad and respective reference monomers, indicating that if electron-transfer quenching occurs, the yield is <0.2 in each case. These findings are consistent with (1) the energy estimates that place the charge-separated state in each case slightly above the excited oxochlorin, with the largest energy gap being for PDI−FbO in toluene (Figure 1), and (2) the transient absorption data, which suggest that a significant fraction of the PDI^- FbO^+ decay occurs by charge recombination to make FbO*, thereby complementing the amount of the excited free base oxochlorin formed by energy transfer from PDI*.

Comparison with Previous Studies. Photoinduced charge-separation processes have been studied previously in arrays containing chlorins/oxochlorins with other tetrapyrrole chromophores,[21,35,36] carotenoids,[18] quinones,[19−25] fullerenes,[26−29] and pyromellitimides.[35,36] In a carotenoid-pheophorbide-quinone triad, electron transfer from the central tetrapyrrole chromophore to the quinone followed by hole transfer to the carotenoid produces a charge-separated state spanning the triad that lives for ∼120 ns.[30] In triads containing a chlorin/oxochlorin plus a porphyrin and either a quinone[21] or pyromellitimide[36] electron acceptor, sequential electron transfer and charge-shift reactions on the time scale of ∼10−100 ps also have been used to generate array-spanning charge-separated states that have lifetimes extending to hundreds of nanoseconds.[21,36] Charge-recombination reactions are generally shorter (∼100 ps to several nanoseconds) in corresponding dyads due to the shorter distance between the oxidized and reduced components.[21,23,26] Rapid (subpicoseconds to hundreds of picoseconds) excited-state electron-transfer followed by slower (subnanoseconds to milliseconds) charge- recombination reactions have been achieved in dyads comprised of chlorins and fullerene.[26a,e,h,27] In many of these systems, like the perylene-oxochlorin dyads studied here, the rates of the charge separation and charge recombination reactions have been manipulated using factors such as solvent polarity and the redox characteristics of the components, including the metalation state of the tetrapyrrole chromophores.

The PDI-containing dyads (PDI−MgO and PDI−ZnO) studied here differ in several respects from the PMI-containing dyad PMI−ZnO studied in the previous paper.[37] The difference in reduction potentials of the PDI and PMI units is the primary factor that facilitates excited-state charge-transfer processes in the former arrays but minimizes these processes in the latter array so that energy-transfer dominates the photodynamics. However, the two types of arrays differ in two other characteristics that may affect perylene-oxochlorin electronic communication (and thus the rates of both through-bond energy and charge transfer if the processes are thermodynamically allowed). First, as described in the preceding article,[37] slightly reduced electronic communication is expected in PMI−ZnO compared to PDI−ZnO (and PDI−MgO and PDI−FbO) because the linker utilizes an ethyne group connected to the meta- versus para-positions of the phenyl ring joined to the perylene. Second, the PMI-based array has the linker connected to the oxochlorin 5-position whereas the PDI-based arrays utilize the 10-position. In principle, differences in electron density at the two oxochlorin sites could affect electronic communication (and thus energy/charge transfer rates) with the perylene. To explore this point, a series of analogous arrays differing only in this connection

motif would need to be prepared and investigated, which is beyond the scope of this study. However, on symmetry grounds one might expect that the orbital coefficients at the oxochlorin 5- and 10-positions are not vastly different. This point seems to be borne out by the fact that the rates of perylene-to-oxochlorin energy transfer are similar ($(3-9\ ps)^{-1}$) in the two types of arrays. These considerations suggest that connection to the 5- versus 10-positions of the oxochlorin makes a far less substantial difference in the excited-state processes than accrues from the use of the different perylene pigments (PMI, PDI).

Conclusions and Outlook

In the preceding article, we showed that incorporation of a perylene-monoimide accessory pigment with an oxochlorin (PMI−ZnO) gives an excellent light-harvesting array in which perylene-to-oxochlorin excited-state energy transfer is essentially quantitative and there is effectively no subsequent quenching of the excited oxochlorin (ZnO*). Here we have shown that perylene-bis(imide) dyes are also excellent light harvesters, transferring energy to the oxochlorin with 35−75% yields in the three dyads PDI−MgO, PDI−ZnO, and PDI−FbO in toluene and benzonitrile. The only reason that perylene-to-oxochlorin energy transfer is not quantitative is because these PDI-containing arrays were designed to bring the charge-separated state ($PDI^-\ O^+$, involving reduced perylene and oxidized oxochlorin) down in energy, thereby facilitating charge-transfer reactions. Indeed, the other fraction of the PDI* that does not undergo energy transfer to make the excited oxochlorin (O*) affords the desired charge-separated state $PDI^-\ O^+$. Thus, in these dyads, the perylene-(bis)imide component serves a dual function: light harvesting and charge separation.

The desired fate of the excited oxochlorin O* (formed either from PDI* or direct excitation) is to subsequently undergo electron transfer to the largest extent possible and thereby generate (additional) $PDI^-\ O^+$. The yield of electron transfer depends very strongly on the oxidation potential of the oxochlorin, which affects the energy of the $PDI^-\ O^+$ state. In PDI−ZnO, we found some potential quenching of ZnO* by the perylene, but not at a level sufficient for a useful charge-separation unit. In the free base analogue PDI−FbO, electron-transfer quenching in the dyad is basically shut off, consistent with the expected higher free energy of the charge-separated state $PDI^-\ FbO^+$ above the excited oxochlorin FbO*. In PDI−MgO, where the energy of $PDI^-\ MgO^+$ drops well below that of MgO*, the yield of oxochlorin-to-perylene electron-transfer rises to ∼70% in toluene and to ∼85% in benzonitrile. When one adds the amount of $PDI^-\ MgO^+$ that is made from PDI* when the accessory pigment is excited (in addition to energy transfer to make MgO*), the overall yield of the charge-separated state elevates to 88% in toluene and 95% in benzonitrile, thereby producing the desired photoproduct in high yield. Furthermore, $PDI^-\ MgO^+$ has a lifetime ≥1 ns in both polar and nonpolar media, making the state suitable for injecting charge into another stage, or substrate, or acting as a molecular-switching unit that can interrupt excited-state energy flow in an adjoining molecular wire. Collectively, the studies described in this paper and the preceding article have provided a set of fully characterized perylene-oxochlorin dyads and have elucidated design criteria that can be exploited for a variety of applications in solar energy and molecular photonics.

Experimental Section

General. ^{1}H NMR (400 MHz) spectra were recorded in $CDCl_3$ unless noted otherwise. Mass spectra were obtained by high-resolution fast atom bombardment mass spectrometry (FAB-MS) and by laser desorption mass spectrometry (LD-MS) in the absence of a matrix.[39] Absorption and emission spectra were collected in toluene at room temperature unless noted otherwise. Silica gel (Baker, 40 μm average particle size) was used for column chromatography. Alumina activity grade I (Fisher) was deactivated to grade V for chromatography of magnesium-porphyrinic compounds.[40] Preparative SEC was performed using BioRad Bio-Beads SX-1 (200−400 mesh) beads. Analytical SEC was performed using a 1000 Å column (flow rate = 0.800 mL/min; solvent = THF; quantitation at 420 and 520 nm; reference at 475 and 590, respectively; oven temperature 40 °C; or quantitation at 520 and 610 nm; reference at 575 and 670, respectively; oven temperature 25 °C). Toluene and triethylamine were freshly distilled from CaH_2 and sparged of oxygen prior to use. All other solvents were used as received. Chloroform contained ethanol (0.8%) as a stabilizer.

10-[4-Ethynylphenyl]-17,18-dihydro-18,18-dimethyl-5-(4-methylphenyl)-17-oxoporphinatozinc(II) (ZnO1). Following a literature method,[16] a solution of Zn1[13,14] (98.2 mg, 165 μmol) and basic alumina (activity I, 7.5 g) in 6 mL toluene was stirred for 16 h at 60 °C in an air atmosphere. TLC analysis of the reaction mixture showed that all of the starting material was consumed. The alumina was concentrated by filtration and was washed with CH_2Cl_2/CH_3OH (19:1) until the washings were colorless, then the filtrate was removed under vacuum. The residue was dissolved in 80 mL of toluene and 2 equiv of DDQ (75.0 mg, 331 μmol) was added. The mixture was stirred for 5 min and then 0.1 mL of triethylamine was added. The solvent was removed under vacuum. Chromatography of the residue (silica, CH_2Cl_2) afforded a bluish-purple solid (46.9 mg, 47%): ^{1}H NMR δ: 2.06 (s, 6H), 2.68 (s, 3H), 3.30 (s, 1H), 7.50−7.54 (m, 2H), 7.84−7.86 (m, 2H), 7.95−7.98 (m, 2H), 8.05−8.08 (m, 2H), 8.58 (d, J = 4.4 Hz, 1H), 8.61 (d, J = 4.4 Hz, 1H), 8.76 (d, J = 4.4 Hz, 1H), 8.86 (d, J = 4.4 Hz, 1H), 8.93 (d, J = 4.4 Hz, 1H), 8.96−9.00 (m, 2H), 9.60 (s, 1H). LD-MS observed: 604.80. FAB-MS observed: 606.1404. Calcd: 606.1398 ($C_{37}H_{26}N_4OZn$). λ_{abs} (log ϵ)/nm 424 (5.48), 563 (3.99), and 609 (4.73).

10-[4-Ethynylphenyl]-17,18-dihydro-18,18-dimethyl-5-(4-methylphenyl)-17-oxoporphyrin (FbO1). A solution of ZnO1 (9.1 mg, 15 μmol) in CH_2Cl_2 (1 mL) was treated with TFA (12 μL, 150 μmol). The reaction mixture was stirred at room temperature and monitored by absorption spectroscopy. After 2 h, the reaction mixture was diluted with CH_2Cl_2 and washed with saturated aqueous $NaHCO_3$. The organic layer was dried (Na_2SO_4) and concentrated. Chromatography on silica (CH_2Cl_2) afforded a purple solid (7.6 mg, 94%): ^{1}H NMR δ: −2.44 to −2.41 (br, 1H), −2.29 to −2.26 (br, 1H), 2.11 (s, 6H), 2.70 (s, 3H), 3.32 (s, 1H), 7.55 (d, J = 7.6 Hz, 2H), 7.86−7.90 (m, 2H), 8.00−8.04 (m, 2H), 8.10−8.14 (m, 2H), 8.60 (d, J = 4.4 Hz, 1H), 8.63 (d, J = 4.4 Hz, 1H), 8.88 (d, J = 4.4 Hz, 1H), 8.96 (d, J = 4.4 Hz, 1H), 9.08−9.10 (m, 1H), 9.15−9.18 (m, 1H), 9.24 (s, 1H), 9.86 (s, 1H). LD-MS observed: 543.14. FAB-MS observed: 544.2233. Calcd: 544.2263 ($C_{37}H_{28}N_4O$). λ_{abs} 416, 512, 548, 593, and 642 nm.

10-[4-Ethynylphenyl]-17,18-dihydro-18,18-dimethyl-5-(4-methylphenyl)-17-oxoporphinatomagnesium(II) (MgO1). Following a standard procedure,[38] a solution of FbO1 (7.1 mg, 13 μmol) in CH_2Cl_2 (1 mL) was treated with DIEA (46 μL, 260 μmol) and MgI_2 (36 mg, 13 μmol). The reaction mixture was stirred at room temperature and monitored by fluorescence

excitation spectroscopy. After 10 min, another batch of MgI_2 (36 mg, 13 μmol) was added and the reaction mixture was stirred for 30 min. Then the reaction mixture was diluted with $CHCl_3$ and washed with saturated aqueous $NaHCO_3$. The organic layer was dried (Na_2SO_4) and concentrated. Chromatography [basic alumina, grade V, $CHCl_3$/methanol (98:2)] afforded a green solid (6.8 mg, 92%): ^{1}H NMR (THF-d_8) δ: 2.03 (s, 6H), 2.67 (s, 3H), 3.77 (s, 1H), 7.52 (d, J = 7.6 Hz, 2H), 7.82 (d, J = 8.0 Hz, 2H), 7.97 (d, J = 8.0 Hz, 2H), 8.09 (d, J = 8.4 Hz, 2H), 8.40−8.45 (m, 2H), 8.62 (d, J = 4.4 Hz, 1H), 8.66 (d, J = 4.4 Hz, 1H), 8.83 (d, J = 4.4 Hz, 1H), 8.91 (d, J = 4.4 Hz, 1H), 8.95 (s, 1H), 9.46 (s, 1H). LD-MS observed: 566.26. FAB-MS observed: 566.1965. Calcd 566.1957 ($C_{37}H_{26}MgN_4O$). λ_{abs} 426, 567, and 616 nm.

***N*-(4-[2-[4-[17,18-Dihydro-18,18-dimethyl-5-(4-methylphenyl)-17-oxoporphinatozinc(II)-10-yl]phenyl]ethynyl]phenyl)-*N*′-(2,5-di-*tert*-butylphenyl)-3,4,9,10-perylene-bis(dicarboximide) (PDI−ZnO).** Following a standard procedure,[2,3] samples of ZnO1 (30.4 mg, 50.0 μmol), PDI-2[6] (39.0 mg, 50.0 μmol), $Pd_2(dba)_3$ (7.3 mg, 8.0 μmol), and P(*o*-tol)$_3$ (19.5 mg, 64.0 μmol) were placed in a Schlenk flask and pump-filled with argon three times. A solution of toluene/triethylamine [21 mL (5:1)] was then added. The mixture was heated to 35 °C. After 4 h, another identical batch of catalyst was added. The reaction was continued for another 7 h. The reaction mixture was cooled to room temperature and filtered through a pad of Celite. The Celite was washed with $CHCl_3$ until the washings were colorless. The filtrate was concentrated under reduced pressure to afford a dark purple solid. Purification was achieved by chromatography [silica, CH_2Cl_2 → CH_2Cl_2/methanol (98:2)], preparative SEC (THF), and chromatography [short silica column, CH_2Cl_2/methanol (98:2)]. The resulting solid was washed with methanol, affording a brown-purple solid (32 mg, 51%): ^{1}H NMR δ 1.31 (s, 9H), 1.35 (s, 9H), 2.06 (s, 6H), 2.69 (s, 3H), 7.07−7.09 (m, 1H), 7.41 (d, J = 8.0 Hz, 2H), 7.45−7.51 (m, 1H), 7.54 (d, J = 8.0 Hz, 2H), 7.60−7.63 (m, 1H), 7.88 (d, J = 8.0 Hz, 2H), 7.94 (d, J = 8.0 Hz, 2H), 7.98 (d, J = 8.0 Hz, 2H), 8.11 (d, J = 8.0 Hz, 2H), 8.55−8.66 (m, 6H), 8.66−8.70 (m, 2H), 8.73−8.76 (m, 2H), 8.81 (d, J = 4.4 Hz, 1H), 8.85 (d, J = 4.0 Hz, 1H), 8.92 (d, J = 4.4 Hz, 1H), 8.96 (s, 1H), 8.98 (d, J = 4.4 Hz, 1H), 9.59 (s, 1H). LD-MS observed: 1255.87. FAB-MS observed: 1258.37. Calcd: 1258.38 ($C_{81}H_{58}N_6O_5Zn$). λ_{abs} 424, 459, 491, 528, 561, and 609 nm.

***N*-(4-[2-[4-[17,18-Dihydro-18,18-dimethyl-5-(4-methylphenyl)-17-oxoporphin-10-yl]phenyl]ethynyl]phenyl)-*N*′-(2,5-di-*tert*-butylphenyl)-3,4,9,10-perylene-bis(dicarboximide) (PDI−FbO).** A solution of PDI−ZnO (9.5 mg, 7.5 μmol) in CH_2Cl_2 (500 μL) was treated with TFA (3.0 μL, 38 μmol). The reaction mixture was stirred at room temperature and monitored by absorption spectroscopy. After 30 min, the reaction mixture was diluted with ethyl acetate and washed with saturated aqueous $NaHCO_3$. The organic layer was dried (Na_2SO_4) and concentrated. Chromatography on silica ($CHCl_3$/methanol, 98:2) afforded a purple solid (5.4 mg, 76%): ^{1}H NMR δ: −2.44 to −2.39 (br, 1H), −2.28 to −2.24 (br, 1H), 1.28−1.38 (m, 18H), 2.12 (s, 6H), 2.72 (s, 3H), 7.06−7.08 (m, 1H), 7.40−7.50 (m, 3H), 7.54 (d, J = 7.6 Hz, 2H), 7.60−7.70 (m, 1H), 7.90 (d, J = 7.6 Hz, 2H), 7.98 (d, J = 7.6 Hz, 2H), 8.04 (d, J = 7.6 Hz, 2H), 8.19 (d, J = 8.0 Hz, 2H), 8.60−8.85 (m, 10H), 8.94 (d, J = 4.4 Hz, 1H), 8.97 (d, J = 4.4 Hz, 1H), 9.10 (d, J = 4.4 Hz, 1H), 9.20 (d, J = 4.4 Hz, 1H), 9.24 (s, 1H), 9.86 (s, 1H). LD-MS observed: 1195.65. FAB-MS observed: 1196.47. Calcd: 1196.46 ($C_{81}H_{60}N_6O_5$). λ_{abs} 417, 460, 492, 528, 589, and 643 nm.

***N*-(4-[2-[4-[17,18-Dihydro-18,18-dimethyl-5-(4-methylphenyl)-17-oxoporphinatomagnesium(II)-10-yl]phenyl]ethynyl]-phenyl)-*N*′-(2,5-di-*tert*-butylphenyl)-3,4,9,10-perylene-bis-(dicarboximide) (PDI−MgO).** Following a standard procedure,[38] a solution of PDI−FbO (4.0 mg, 3.3 μmol) in CH_2Cl_2 (500 μL) was treated with DIEA (23 μL, 130 μmol) and MgI_2 (18 mg, 6.6 μmol). The reaction mixture was stirred at room temperature and monitored by fluorescence excitation spectroscopy. After 3 h, the fluorescence excitation spectrum of a sample from the reaction mixture showed the presence of PDI−FbO. Therefore, the reaction mixture was stirred overnight. Then, the reaction mixture was diluted with $CHCl_3$ and washed with saturated aqueous $NaHCO_3$. The organic layer was dried (Na_2SO_4) and concentrated. Chromatography (basic alumina, grade V, $CHCl_3$) afforded a purple solid (1.8 mg, 45%): ^{1}H NMR (THF-d_8) δ: 1.25−1.32 (m, 18H), 2.03 (s, 6H), 2.70 (s, 3H), 7.28−7.30 (m, 1H), 7.40−7.45 (m, 2H), 7.50−7.65 (m, 4H), 7.82 (d, J = 7.6 Hz, 2H), 7.93 (d, J = 7.6 Hz, 2H), 7.98 (d, J = 7.6 Hz, 2H), 8.16 (d, J = 7.6 Hz, 2H), 8.48 (d, J = 4.4 Hz, 1H), 8.51 (d, J = 4.4 Hz, 1H), 8.60−8.70 (m, 6H), 8.75−8.85 (m, 5H), 8.92 (d, J = 4.4 Hz, 1H), 8.95 (s, 1H), 9.47 (s, 1H). LD-MS observed: 1219.92. FAB-MS observed: 1218.42. Calcd: 1218.43 ($C_{81}H_{58}MgN_6O_5$). λ_{abs} 427, 460, 492, 528, 589, and 617 nm.

Characterization. The electrochemical and spectroscopic studies were conducted using instrumentation and techniques previously described.[5] Transient absorption measurements used 5−10 mM samples at room-temperature excited with ∼130 fs, 20−30 mJ, and 480−600 nm pulses.

Acknowledgment. This research was supported by the NSF (CHE-9988142). Mass spectra were obtained at the Mass Spectrometry Laboratory for Biotechnology at North Carolina State University. Partial funding for the Mass Spectrometry Laboratory for Biotechnology at North Carolina State University was obtained from the North Carolina Biotechnology Center and the National Science Foundation.

Supporting Information Available: Complete spectral data (absorption, ^{1}H NMR, and LD-MS) for all new compounds. This material is available free of charge via the Internet at http://pubs.acs.org.

References and Notes

(1) Holten, D.; Bocian, D. F.; Lindsey, J. S. *Acc. Chem. Res.* **2002**, *35*, 57−69.

(2) Wagner, R. W.; Johnson, T. E.; Li, F.; Lindsey, J. S. *J. Org. Chem.* **1995**, *60*, 5266−5273.

(3) Wagner, R. W.; Ciringh, Y.; Clausen, C.; Lindsey, J. S. *Chem. Mater.* **1999**, *11*, 2974−2983.

(4) Miller, M. A.; Lammi, R. K.; Prathapan, S.; Holten, D.; Lindsey, J. S. *J. Org. Chem.* **2000**, *65*, 6634−6649.

(5) Prathapan, S.; Yang, S. I.; Seth, J.; Miller, M. A.; Bocian, D. F.; Holten, D.; Lindsey, J. S. *J. Phys. Chem. B* **2001**, *105*, 8237−8248.

(6) Yang, S. I.; Prathapan, S.; Miller, M. A.; Seth, J.; Bocian, D. F.; Lindsey, J. S.; Holten, D. *J. Phys. Chem. B* **2001**, *105*, 8249−8258.

(7) Yang, S. I.; Lammi, R. K.; Prathapan, S.; Miller, M. A.; Seth, J.; Diers, J. R.; Bocian, D. F.; Lindsey, J. S.; Holten, D. *J. Mater. Chem.* **2001**, *11*, 2420−2430.

(8) Ambroise, A.; Kirmaier, C.; Wagner, R. W.; Loewe, R. S.; Bocian, D. F.; Holten, D.; Lindsey, J. S. *J. Org. Chem.* **2002**, *67*, 3811−3826.

(9) Kirmaier, C.; Yang, S. I.; Prathapan, S.; Miller, M. A.; Diers, J. R.; Bocian, D. F.; Lindsey, J. S.; Holten, D. *Res. Chem. Intermed.* **2002**, *28*, 719−740.

(10) (a) Loewe, R. S.; Chevalier, F.; Tomizaki, K.-Y.; Lindsey, J. S. *J. Porphyrins Phthalocyanines.* In press. (b) Kirmaier, C.; Schwartz, J. K.; Hindin, E.; Diers, J. R.; Loewe, R. S.; Tomizaki, K.-Y.; Birge, R. R.; Bocian, D. F.; Lindsey, J. S.; Holten, D. Manuscripts in preparation.

(11) Tomizaki, K.-Y.; Loewe, R. S.; Kirmaier, C.; Schwartz, J. K.; Retsek, J. L.; Bocian, D. F.; Holten, D.; Lindsey, J. S. *J. Org. Chem.* **2002**, *12*, 3438−3451.

(12) Loewe, R. S.; Tomizaki, K.-Y.; Youngblood, W. J.; Bo, Z.; Lindsey, J. S. *J. Mater. Chem.* **2002**, *12*, 3438−3451.

(13) Taniguchi, M.; Ra, D.; Mo, G.; Balasubramanian, T.; Lindsey, J. S. *J. Org. Chem.* **2001**, *66*, 7342−7354.

(14) (a) Strachan, J.-P.; O'Shea, D. F.; Balasubramanian, T.; Lindsey, J. S. *J. Org. Chem.* **2000**, *65*, 3160−3172. (b) Strachan, J.-P.; O'Shea, D. F.; Balasubramanian, T.; Lindsey, J. S. *J. Org. Chem.* **2001**, *66*, 642.

(15) Balasubramanian, T.; Strachan, J.-P.; Boyle, P. D.; Lindsey, J. S. *J. Org. Chem.* **2000**, *65*, 7919−7929.

(16) Taniguchi, M.; Kim, H.-J.; Ra, D.; Schwartz, J. K.; Kirmaier, C, Hindin, E.; Diers, J. R.; Prathapan, S.; Bocian, D. F.; Holten, D.; Lindsey, J. S. *J. Org. Chem.* **2002**, *67*, 7329−7342.

(17) (a) Montforts, F.-P.; Gerlach, B.; Höper, F. *Chem. Rev.* **1994**, *94*, 327−347. (b) Jacobi, P. A.; Lanz, S.; Ghosh, I.; Leung, S. H.; Löwer, F.; Pippin, D. *Org. Lett.* **2001**, *3*, 831−834. (c) Silva, A. M. G.; Tomé, A. C.; Neves, M. G. P. M. S.; Cavaleiro, J. A. S. *Tetrahedron Lett.* **2000**, *41*, 3065−3068. (d) Shea, K. M.; Jaquinod, L.; Khoury, R. G.; Smith, K. M. *Tetrahedron.* **2000**, *56*, 3139−3144. (e) Burns, D. H.; Shi, D. C.; Lash, T. D. *Chem. Commun.* **2000**, 299−300. (f) Krattinger, B.; Callot, H. J. *Eur. J. Org. Chem.* **1999**, 1857−1867. (g) Johnson, C. K.; Dolphin, D. *Tetrahedron Lett.* 1998, *39*, 4619−4622. (h) Mironov, A. F.; Efremov, A. V.; Efremova, O. A.; Bonnett, R.; Martinez, G. *J. Chem. Soc., Perkin Trans. 1* **1998**, 3601−3608.

(18) Liddell, P. A.; Nemeth, G. A.; Lehman, W. R.; Joy, A. M.; Moore, A. L.; Bensasson, R. V.; Moore, T. A.; Gust, D. *Photochem. Photobiol.* **1982**, *36*, 641−645.

(19) Lindsey, J. S.; Delaney, J. K.; Mauzerall, D. C.; Linschitz, H. *J. Am. Chem. Soc.* **1988**, *110*, 3610−3621.

(20) (a) Wasielewski, M. R. *Chem. Rev.* **1992**, *92*, 435−461. (b) Wasielewski, M. R. In *Chlorophylls*; Scheer, H., Ed.; CRC Press: Boca Raton, FL, 1991; pp 269−286.

(21) (a) Johnson, D. G.; Niemczyk, M. P.; Minsek, D. W.; Wiederrecht, G. P.; Svec, W. A.; Gaines, G. L. III; Wasielewski, M. R. *J. Am. Chem. Soc.* **1993**, *115*, 5692−5701. (b) Wasielewski, M. R.; Wiederrecht, G. P.; Svec, W. A.; Niemczyk, M. P. *Solar Energy Mater. Solar Cells* **1995**, *38*, 127−134.

(22) (a) Abel, Y.; Montforts, F.-P. *Tetrahedron Lett.* **1997**, *38*, 1745−1748. (b) Kutzki, O.; Montforts, F.-P. *Synlett* **2001**, 53−56.

(23) Tkachenko, N. V.; Tauber, A. Y.; Grandell, D.; Hynninen, P. H.; Lemmetyinen, H. *J. Phys. Chem. A* **1999**, *103*, 3646−3656.

(24) Malinen, P. K.; Tauber, A. Y.; Helaja, J.; Hynninen, P. H. *Liebigs Ann.* **1997**, 1801−1804.

(25) Mössler, H.; Wittenberg, M.; Niethammer, D.; Mudrassagam, R. K.; Kurreck, H.; Huber, M. *Magn. Reson. Chem.* **2000**, *38*, 67−84.

(26) (a) Tkachenko, N. V.; Rantala, L.; Tauber, A. Y.; Helaja, J.; Hynninen, P. H.; Lemmetyinen, H. *J. Am. Chem. Soc.* **1999**, *121*, 9378−9387. (b) Helaja, J.; Tauber, A. Y.; Abel, Y.; Tkachenko, N. V.; Lemmetyinen, H., Kilpeläinen, I.; Hynninen, P. H. *J. Chem. Soc., Perkin Trans. 1* **1999**, *121*, 2403−2408. (c) Tkachenko, N. V.; Vuorimaa, E.; Kesti, T.; Alekseev, A. S.; Tauber, A. Y.; Hynninen, P. H.; Lemmetyinen, H. *J. Phys. Chem B* **2000**, *104*, 6371−6379. (d) Tkachenko, N. V.; Guenther, C.; Imahori, H.; Tamaki, K.; Sakata, Y.; Shunichi, F.; Lemmetyinen, H. *Chem. Phys. Lett.* **2000**, 326, 344−350. (e) Vehmanen, V.; Tkachenko, N. V.; Tauber, A. Y.; Hynninen, P. H.; Lemmetyinen, H. *Chem. Phys. Lett.* **2001**, *345*, 213-218. (f) Efimov, A.; Tkachenko, N. V.; Lemmetyinen, H. *J. Porphyrins Phthalocyanines* **2001**, 5, 835−838. (g) Alekseev, A. S.; Tkachenko, N. V.; Tauber, A. Y.; Hynninen, P. H.; Osterbacka, R.; Stubb, H.; Lemmetyinen, H. *Chem. Phys.* **2002**, 275, 243−251. (h) Vehmanen, V.; Tkachenko, N. V.; Efimov, A.; Damlin, P.; Ivaska, A.; Lemmetyinen, H. *J. Phys. Chem. A* **2002**, *106*, 8029−8038.

(27) Zheng, G.; Dougherty, T. J.; Pandey, R. K. *Chem. Commun.* **1999**, 2469−2470.

(28) Fukuzumi, S.; Ohkubo, K.; Imahori, H.; Shao, J.; Ou, Z.; Zheng, G.; Chen, Y.; Pandey, R. K.; Fujitsuka, M.; Ito, O.; Kadish, K. M. *J. Am. Chem. Soc.* **2001**, *123*, 10676−10683.

(29) (a) Kutzki, O.; Walter, A.; Montforts, F.-P. *Helv. Chim. Acta* **2000**, *83*, 2231−2245. (b) Montforts, F.-P.; Kutzki, O. *Angew. Chem. Int. Ed.* **2000**, *39*, 599−601.

(30) Liddell, P. A.; Barrett, D.; Makings, L. R.; Pessiki, P. J.; Gust, D.; Moore, T. A. *J. Am. Chem. Soc.* **1986**, *108*, 5350−5352.

(31) Wasielewski, M. R.; Liddell, P. A.; Barrett, D.; Moore, T. A.; Gust, D. *Nature* **1986**, *322*, 570−572.

(32) Zenkevich, E. I.; Knyukshto, V. N.; Shulga, A. M.; Kuzmitsky, V. A.; Gael, V. I.; Levinson, E. G.; Mironov, A. F. *J. Lumin.* **1997**, *75*, 229−244.

(33) Tamiaki, H.; Miyatake, T.; Tanikaga, R.; Holzwarth, A. R.; Schaffner, K. *Angew. Chem. Int. Ed.* **1996**, *35*, 772−774.

(34) (a) Osuka, A.; Wada, Y.; Maruyama, K.; Tamiaki, H. *Heterocycles* **1997**, *44*, 165−168. (b) Osuka, A.; Marumo, S.; Maruyama, K. *Bull. Chem. Soc. Jpn.* **1993**, *66*, 3837−3839.

(35) Osuka, A.; Marumo, S.; Maruyama, K.; Mataga, N.; Tanaka, Y.; Taniguchi, S.; Okada, T.; Yamazaki, I.; Nishimura, Y. *Bull. Chem. Soc. Jpn.* **1995**, *68*, 262−276.

(36) Osuka, A.; Marumo, S.; Mataga, N.; Taniguchi, S.; Okada, T.; Yamazaki, I.; Nishimura, Y.; Ohno, T.; Nozaki, K. *J. Am. Chem. Soc.* **1996**, *118*, 155−168.

(37) Muthukumaran, K.; Loewe, R. S.; Kirmaier, C.; Hindin, E.; Schwartz, J. K.; Sazanovich, I. V.; Diers, J. R.; Bocian, D. F.; Holten, D.; Lindsey, J. S. *J. Phys. Chem. B* **2003**, *107*, 3431.

(38) Lindsey, J. S.; Woodford, J. N. *Inorg. Chem.* **1995**, *34*, 1063−1069.

(39) (a) Fenyo, D.; Chait, B. T.; Johnson, T. E.; Lindsey, J. S. *J. Porphyrins Phthalocyanines* **1997**, *1*, 93−99. (b) Srinivasan, N.; Haney, C. A.; Lindsey, J. S.; Zhang, W.; Chait, B. T. *J. Porphyrins Phthalocyanines* **1999**, *3*, 283−291.

(40) Li, F.; Gentemann, S.; Kalsbeck, W. A.; Seth, J.; Lindsey, J. S.; Holten, D.; Bocian, D. F. *J. Mater. Chem.* **1997**, *7*, 1245−1262.

(41) Seybold, P. G.; Gouterman, M. *J. Mol. Spectrosc.* **1969**, *31*, 1−13.